Boulder School for
Condensed Matter and Materials Physics

Laurette Tuckerman
PMMH-ESPCI-CNRS
laurette@pmmh.espci.fr

Hydrodynamic Instabilities:

Convection and Lorenz Model

Web sites used in demonstrations

Lorenz model:
http://www.cmp.caltech.edu/~mcc/Chaos_Course
http://en.wikipedia.org/wiki/Lorenz_attractor http://to-campos.planetaclix.pt/fractal/lorenz_eng.html
http://people.web.psi.ch/gassmann/waterwheel/Wwheel1.HTML
Spiral defect chaos:
http://www.youtube.com/watch?v=DxQ1BjQcicg

1 Convection

The chapter is devoted to the study of a fluid layer between two plates maintained at different temperatures. If the lower plate is significantlyy hotter than the upper plate, this will lead to fluid motion.

1.1 Rayleigh criterion

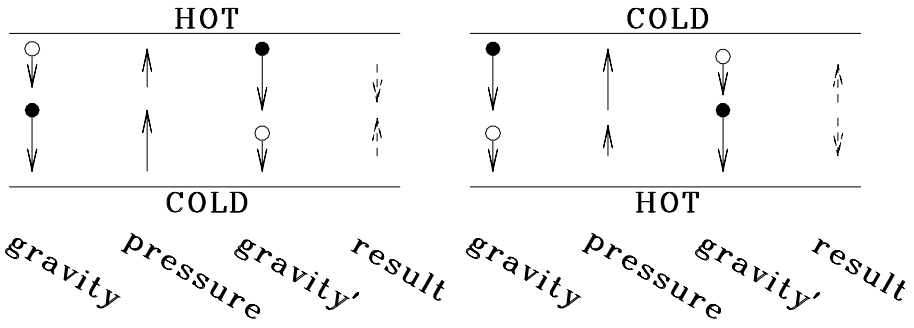

Figure 1: Mechanism of convective instability. The gravitational and the pressure forces counterbalance one another. If a particle is displaced while retaining its temperature and therefore its density, then the two forces wil not counterbalance one another. If the cold plate is below and the hot plate above, then the difference between the two forces will be directed in such a way as to oppose the displacement, meaning that the original situation is stable. In the case of the reverse configuration, then the differences between the two forces will tend to amplify the displacement, leading to instability.

The fundamental physical mechanism can be understood by an argument due to Rayleigh regarding inviscid fluids. This mechanism is illustrated in figure 1. In the fluid layer, a vertical pressure gradient is established which exactly counterbalances gravity. The gravitational force in turn depends on the local density (we assume that the dependence on the distance from the center of the earth is negligible compared to the dependence on density). Now imagine displacing vertically a fluid particle. In the absence of viscosity or thermal diffusivity, the particle retains its original temperature, and hence the gravitational force acting on it remains the same. However, at its new height, the ambient pressure gradient is different and there is no longer equlibrium between the two forces. There are two possible cases. If the resulting force is such as to send the particle back to its original height, then the original stratification is stable. This is the case when the density decreases with height. If, on the other hand, the resulting force is such as to send the fluid further in the direction of the displacement, then the original stratification is unstable. This is the case when the density increases with height.

We will begin by stating the continuum equations which govern the coupled velocity and temperature fields, called the Boussinesq equations. With additional hypotheses, we will simplify these equations in

order to carry out a linear stability analysis.

1.2 Boussinesq Approximation

The Boussinesq approximation consists of assuming that all of the fluid properties, in particular the diffusivity of momentum (viscosity) μ et and temperature κ, and the density ρ, are constant and uniform, except in the buoyancy force which generates convection, where the density is assumed to vary linearly with temperature:

$$\rho(T) = \rho_0 \left[1 - \alpha(T - T_0)\right] \tag{1}$$

These approximations are valid when the difference $T_0 - T_1$ between the two temperatures is not too large. The resulting equations are:

$$\begin{aligned} \rho_0 \left[\partial_t + (U \cdot \nabla)\right] U &= -\nabla P - g\rho(T)\mathbf{e_z} + \mu \Delta U && \text{(2a)} \\ \nabla \cdot U &= 0 && \text{(2b)} \\ \left[\partial_t + (U \cdot \nabla)\right] T &= \kappa \Delta T && \text{(2c)} \end{aligned}$$

with boundary conditions

$$\begin{aligned} \mathbf{U} &= 0 \text{ at } z = 0, d && \text{(2d)} \\ T &= T_0 \text{ at } z = 0, \quad T = T_1 \text{ at } z = d && \text{(2e)} \end{aligned}$$

where $\mathbf{U}$ is the velocity vield, T the temperature field P the pressure, g the gravitational acceleration, μ the viscosity and κ the thermal diffusivity. The terms in $\mathbf{U} \cdot \nabla$ describe the *l'advection*: even without any forces, the velocity and temperature fields evolve due to the fluid motion that transports them. The terms in Δ describe the diffusion of momentum or of temperature. The equation $\nabla \cdot \mathbf{U} = 0$ describes incompressibility, or, rather, the version of it implied by the Boussinesq approximation.

1.3 Calculation and subtraction of the basic state

System (2) has one very simple solution:

$$\begin{aligned} \text{motionless:} \quad & \mathbf{U}^* = 0 && \text{(3a)} \\ \text{uniform temperature gradient:} \quad & T^* = T_0 - (T_0 - T_1)\tfrac{z}{d} && \text{(3b)} \\ \text{hydrostatic pressure:} \quad & P^* = P_0 - dg\rho_0 \left[\tfrac{z}{d} + \tfrac{\alpha}{2}(T_0 - T_1)\left(\tfrac{z}{d}\right)^2\right] && \text{(3c)} \end{aligned}$$

In (3), a pressure field is established which exactly counterbalances the buoyancy force, just as the usual hydrostatic pressure counterbalances the usual gravitational force.

$$-\nabla P^* - g\rho(T^*) = 0 \tag{4}$$

We now introduce variables measuring the deviations from the basic state (3):

$$T = T^* + \hat{T} \quad P = P^* + \hat{P} \tag{5}$$

Using the calculations

$$\begin{aligned}
\rho(T^* + \hat{T}) &= \rho_0(1 - \alpha(T^* + \hat{T} - T_0)) \\
&= \rho_0(1 - \alpha(T^* - T_0)) - \rho_0\alpha\hat{T} = \rho(T^*) - \rho_0\alpha\hat{T} \\
-\nabla P - g\rho(T)\mathbf{e_z} &= -\nabla P^* - g\rho(T^*) - \nabla\hat{P} + g\rho_0\alpha\hat{T}\mathbf{e_z} \\
(\mathbf{U}\cdot\nabla)T &= (\mathbf{U}\cdot\nabla)T^* + (\mathbf{U}\cdot\nabla)\hat{T} \\
&= (\mathbf{U}\cdot\nabla)\left(T_0 - (T_0 - T_1)\frac{z}{d}\right) + (\mathbf{U}\cdot\nabla)\hat{T} \\
&= -\frac{T_0 - T_1}{d}\mathbf{U}\cdot\mathbf{e_z} + (\mathbf{U}\cdot\nabla)\hat{T}
\end{aligned}$$

we replace equations (2) by

$$\rho_0\left[\partial_t + (\mathbf{U}\cdot\nabla)\right]\mathbf{U} = -\nabla\hat{P} + g\rho_0\alpha\hat{T}\mathbf{e_z} + \mu\Delta\mathbf{U} \tag{6a}$$

$$\nabla\cdot\mathbf{U} = 0 \tag{6b}$$

$$\left[\partial_t + (\mathbf{U}\cdot\nabla)\right]\hat{T} = \frac{T_0 - T_1}{d}\mathbf{U}\cdot\mathbf{e_z} + \kappa\Delta\hat{T} \tag{6c}$$

with homogeneous boundary conditions

$$\mathbf{U} = 0 \text{ at } z = 0, d \tag{6d}$$

$$\hat{T} = 0 \text{ at } z = 0, d \tag{6e}$$

1.4 Nondimensionalisation

By choosing the scales

$$z = d\bar{z}, \quad t = \frac{d^2}{\kappa}\bar{t}, \quad \mathbf{U} = \frac{\kappa}{d}\bar{\mathbf{U}}, \quad \hat{T} = \frac{\mu\kappa}{d^3 g\rho_0\alpha}\bar{T}, \quad \hat{P} = \frac{\rho_0\mu\kappa}{\rho_0 d^2}\bar{P} \tag{7}$$

and introducing them into equations (6),

$$\frac{\kappa}{d^2}\frac{\kappa}{d}\rho_0\left[\partial_{\bar{t}} + (\bar{\mathbf{U}}\cdot\bar{\nabla})\right]\bar{\mathbf{U}} = -\frac{1}{d}\frac{\rho_0\mu\kappa}{\rho_0 d^2}\bar{\nabla}\bar{P} + g\rho_0\alpha\frac{\mu\kappa}{d^3 g\rho_0\alpha}\bar{T}\mathbf{e_z} + \mu\frac{1}{d^2}\frac{\kappa}{d}\bar{\Delta}\bar{\mathbf{U}} \tag{8a}$$

$$\frac{1}{d}\frac{\kappa}{d}\bar{\nabla}\cdot\bar{\mathbf{U}} = 0 \tag{8b}$$

$$\frac{\kappa}{d^2}\frac{\mu\kappa}{d^3 g\rho_0\alpha}\left[\partial_{\bar{t}} + (\bar{\mathbf{U}}\cdot\bar{\nabla})\right]\bar{T} = \frac{\kappa}{d}\frac{T_0 - T_1}{d}\bar{\mathbf{U}}\cdot\mathbf{e_z} + \kappa\frac{1}{d^2}\frac{\mu\kappa}{d^3 g\rho_0\alpha}\bar{\Delta}\bar{T} \tag{8c}$$

as well as the kinematic viscosity $\nu = \mu/\rho_0$, we obtain:

$$\left[\partial_{\bar{t}} + (\bar{\mathbf{U}} \cdot \bar{\nabla})\right] \bar{\mathbf{U}} = \frac{\nu}{\kappa}\left[-\bar{\nabla}\bar{P} + \bar{T}\mathbf{e_z} + \bar{\Delta}\bar{\mathbf{U}}\right] \tag{9a}$$

$$\bar{\nabla} \cdot \bar{\mathbf{U}} = 0 \tag{9b}$$

$$\left[\partial_{\bar{t}} + (\bar{\mathbf{U}} \cdot \bar{\nabla})\right] \bar{T} = \frac{(T_0 - T_1)d^3 g\alpha}{\kappa\nu}\bar{\mathbf{U}} \cdot \mathbf{e_z} + \bar{\Delta}\bar{T} \tag{9c}$$

The nondimensional parameters appearing in (9) are:

$$\text{the Prandtl number:} \qquad Pr \equiv \frac{\nu}{\kappa} \tag{10}$$

$$\text{the Rayleigh number:} \qquad Ra \equiv \frac{(T_0 - T_1)d^3 g\alpha}{\kappa\nu} \tag{11}$$

The Rayleigh number Ra measures the imposed thermal gradient. It is by increasing Ra that instabilities occur. The Prandtl number Pr is the ratio of the diffusivities of velocity and temperature: for Pr large (small), the temperature (velocity) is more volatile.

1.5 Boundary conditions

We simplify the notation by returning to $\mathbf{U}$, T, z, etc. without overbars and we write $\mathbf{U} = (u, v, w)$. We seek solutions that are periodic in the horizontal direction, with periodicity $2\pi/q$. In the vertical direction, we impose at $z = 0, 1$:

$$T = 0 \qquad \text{perfectly conducting plates} \tag{12a}$$

$$w = 0 \qquad \text{impermeable plates} \tag{12b}$$

Realistic vertical boundary conditions would be

$$u = v = 0 \quad \text{rigid boundaries: zero tangential velocity} \tag{13}$$

Instead of (13), we will instead impose the following condition:

$$\partial_z u + \partial_x w = \partial_z v + \partial_y w = 0 \quad \text{zero tangential stress} \tag{14}$$

Physically, condition (14) would correspond to a free surfaces. But this is difficult to imagine. Without a rigid boundary, first of all, the layer would fall down. Secondly, we could not maintain the surface at a fixed temperature. We will use (14), despite the fact that it is unrealistic, because it greatly simplifies the calculations.

$$w|_{z=0,1} = 0 \Longrightarrow \partial_x w|_{z=0,1} = \partial_y w|_{z=0,1} = 0 \tag{15}$$

which can be combined with (14) to yield

$$\partial_z u = \partial_z v = 0 \tag{16}$$

The advantage of imposing (16) instead of (13) is, as we will see later, that we can use trigonometric functions $\sin(k\pi z)$, which are easy to work with.

1.6 Two-dimensional case

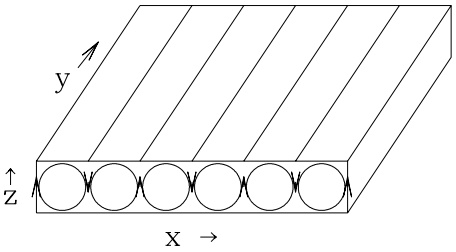

Figure 2: Two-dimensional convection rolls.

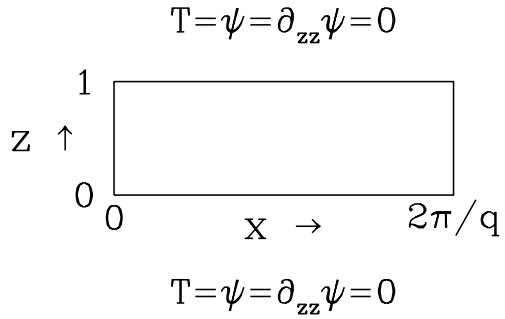

Figure 3: Boundary conditions on T and ψ obtained by imposing horizontal periodicity and zero tangential stress (free surfaces) on the vertical boundaries.

From now on, we will assume that the solution is two-dimensional, i.e. that $\partial_y = 0$. We will also assume that $v = 0$. Visually, the solution consists of infinite straight rolls, oriented along the $\mathbf{e_y}$ axis, as shown in figure 2. We therefore can define the streamfunction ψ such that:

$$\mathbf{U} = \nabla \times \psi \, \mathbf{e_y} \Longrightarrow \left\{ \begin{array}{c} u = -\partial_z \psi \\ w = \partial_x \psi \end{array} \right. \tag{17}$$

The boundary conditions on ψ at $z = 0, 1$ are

$$0 = \partial_z u = -\partial^2_{zz} \psi \tag{18a}$$

$$0 = w = \partial_x \psi \Longrightarrow \left\{ \begin{array}{l} \psi = \psi_1 \text{ at } z = 1 \\ \psi = \psi_0 \text{ à } z = 0 \end{array} \right. \tag{18b}$$

(Note that the realistic condition $u = 0$ at rigid boundaries would have led to $\partial_z \psi = 0$ instead of (18a).)

The value of $\psi_1 - \psi_0$ is the horizontal flux:

$$\int_{z=0}^{1} dz \; u(x,z) = -\int_{z=0}^{1} dz \; \partial_z \psi(x,z) = -\left. \psi(x,z) \right]_{z=0}^{1} = \psi_0 - \psi_1 \tag{19}$$

Since ψ is only defined up to an additive constant, we can set $\psi_0 = 0$. If we then impose a horizontal flux of zero, we obtain

$$\psi_0 = \psi_1 = 0 \tag{20}$$

To use the streamfunction, we compute:

$$\mathbf{U} \cdot \nabla T = u\ \partial_x T + w\ \partial T = -\partial_z \psi\ \partial_x T + \partial_x \psi\ \partial_z T \equiv J[\psi, T] \tag{21}$$

where J is called the Poisson bracket, which yields, for the temperature governing the temperature evolution:

$$\partial_t T + J[\psi, T] = Ra\ \partial_x \psi + \Delta T \tag{22a}$$

In order to eliminate the pressure from the momentum equation, we act on it with $\mathbf{e_y} \cdot \nabla \times$. Let us calculate the required terms:

$$\begin{aligned}
\mathbf{e_y} \cdot \nabla \times \mathbf{U} &= \mathbf{e_y} \cdot \nabla \times \nabla \times \psi \mathbf{e_y} = -\Delta \psi \\
\mathbf{e_y} \cdot \nabla \times \Delta \mathbf{U} &= \mathbf{e_y} \cdot \nabla \times \Delta \nabla \times \psi \mathbf{e_y} = -\Delta^2 \psi \\
\mathbf{e_y} \cdot \nabla \times T \mathbf{e_z} &= -\partial_x T \\
\mathbf{e_y} \cdot \nabla \times (\mathbf{U} \cdot \nabla) \mathbf{U} &= \partial_z (\mathbf{U} \cdot \nabla) u - \partial_x (\mathbf{U} \cdot \nabla) w \\
&= \partial_z (u \partial_x u + w \partial_z u) - \partial_x (u \partial_x w + w \partial_z w) \\
= \partial_z u\ \partial_x u + \partial_z w\ \partial_z u - \partial_x u\ \partial_x w - \partial_x w\ \partial_z w &+ u\ \partial_{xz} u + w\ \partial_{zz} u - u\ \partial_{xx} w - w\ \partial_{xz} w \\
= \partial_z u\ (\partial_x u + \partial_z w) - \partial_x w\ (\partial_x u + \partial_z w) &+ u\ \partial_x (\partial_z u - \partial_x w) + w \partial_z (\ \partial_z u - \partial_x w) \\
= (-\partial_z \psi) \partial_x (-\partial_{zz} \psi - \partial_{xx} \psi) &+ (\partial_x \psi) \partial_z (-\partial_{zz} \psi - \partial_{xx} \psi) \\
&= (\partial_z \psi) \partial_x (\Delta \psi) - (\partial_x \psi) \partial_z (\Delta \psi) \\
&= -J[\psi, \Delta \psi]
\end{aligned}$$

Assembling these terms, we obtain:

$$\partial_t \Delta \psi + J[\psi, \Delta \psi] = Pr[\partial_x T + \Delta^2 \psi] \tag{22b}$$

1.7 Linear stability analysis

Two-dimensional perturbations of a stationary fluid layer with a uniform temperature gradient (the basic solution (3)) evolve according to equations (22a) and (22b). To carry out a stability analysis of the basic state, we neglect terms that are not of linear order in ψ, T (here, the quadratic terms of the Poisson brackets) in (22a) and (22b), writing:

$$\partial_t \Delta \psi = Pr[\partial_x T + \Delta^2 \psi] \tag{23a}$$

$$\partial_t T = Ra\ \partial_x \psi + \Delta T \tag{23b}$$

Solutions of (23) with vertical boundary conditions (18a-20) and horizontal periodic boundary conditions are of the form:

$$\psi(x,z,t) = \hat{\psi}\ \sin qx\ \sin k\pi z\ e^{\lambda t} \quad q \in \mathcal{R},\ k \in \mathcal{Z}^+,\ \lambda \in \mathcal{C} \tag{24a}$$

$$T(x,z,t) = \hat{T}\ \cos qx\ \sin k\pi z\ e^{\lambda t} \tag{24b}$$

(In the left-hand-side of (24), ψ, T are functions of (x,z,t), while in the right-hand-side, $\hat{\psi}$, $\hat{T}$ are scalar coefficients.) Trigonometric or exponential dependence on the variables x, z, t is derived from a very general principle: the equations are linear (in ψ and T) and homogeneous (no explicit dependence and hence no distinguished values) in these three variables. The more specialized form in x, z of (24) is justified by

–periodicity in x with $\psi \sim \partial_x T$ and $T \sim \partial_x \psi$
–the boundary conditions $T = \psi = \partial_{zz}\psi = 0$ at $z = 0, 1$

Using (24) and defining $\gamma^2 \equiv q^2 + (k\pi)^2$, the partial differential equations (23) are transformed into algebraic equations:

$$-\lambda\gamma^2\hat{\psi} = Pr[-q\hat{T} + \gamma^4\hat{\psi}] \tag{25a}$$

$$\lambda\hat{T} = Ra\ q\ \hat{\psi} - \gamma^2\hat{T} \tag{25b}$$

or

$$\lambda \begin{bmatrix} \hat{\psi} \\ \hat{T} \end{bmatrix} = \begin{bmatrix} -Pr\ \gamma^2 & Pr\ q/\gamma^2 \\ Ra\ q & -\gamma^2 \end{bmatrix} \begin{bmatrix} \hat{\psi} \\ \hat{T} \end{bmatrix} \tag{26}$$

Let us seek a *steady* bifurcation, that is, a non-trivial solution of (26) with eigenvalue $\lambda = 0$. This requires that:

$$Pr\,\gamma^4 - Pr\ Ra\ \frac{q^2}{\gamma^2} = 0 \tag{27}$$

and thus that:

$$Ra = \frac{\gamma^6}{q^2} = \frac{(q^2 + (k\pi)^2)^3}{q^2} \equiv Ra_c(q,k) \tag{28}$$

The basic state becomes unstable to perturbations of the form (24) (i.e. $\lambda > 0$) for $Ra > Ra_c(q,k)$. For the basic state to be stable to perturbations for *all* q, k, we require that

$$Ra < \min_{\substack{q \in \mathcal{R} \\ k \in \mathcal{Z}^+}} Ra_c(q,k) \tag{29}$$

$$\begin{aligned} 0 &= \frac{\partial Ra_c(q,k)}{\partial q} = \frac{q^2 3(q^2 + (k\pi)^2)^2 2q - 2q(q^2 + (k\pi)^2)^3}{q^4} \\ &= \frac{2(q^2 + (k\pi)^2)^2}{q^3}(3q^2 - (q^2 + (k\pi)^2) \quad \Longrightarrow \quad q^2 = \frac{(k\pi)^2}{2} \end{aligned} \tag{30}$$

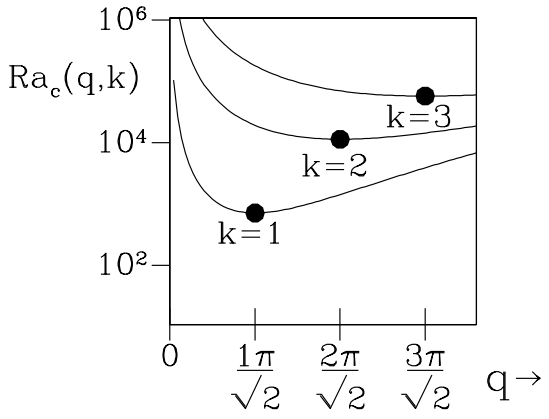

Figure 4: Critical threshold $Ra_c(q,k)$ for $k = 1$, 2, 3.

$$Ra_c\left(q=\frac{k\pi}{\sqrt{2}},k\right)=\frac{(k\pi)^2/2+(k\pi)^2)^3}{(k\pi)^2/2}=\frac{27}{4}(k\pi)^4 \tag{31}$$

The instability threshold is thus:

$$Ra_c = Ra_c\left(q=\frac{\pi}{\sqrt{2}},k=1\right)=\frac{27}{4}(\pi)^4=657.5 \tag{32}$$

This calculation was simplified by the free surface hypothesis (zero tangential stress). The calculation using realistic conditions of rigid plates follows the same principle, but is more complicated. The threshold Ra_c obtained is higher, because rigid boundaries help to damp perturbations. The critical wavenumber q_c decreases, so that the rolls become almost circular: the width ℓ of a roll is π/q.

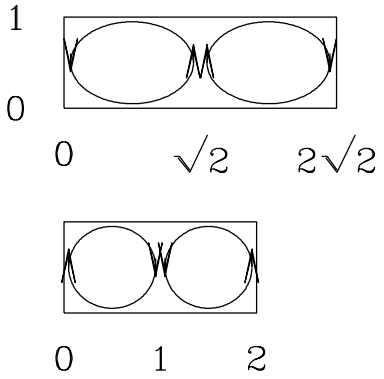

	Ra_c	q_c	ℓ_c
free surfaces	$\frac{27}{4}\pi^4 = 657.5$	$\frac{\pi}{\sqrt{2}}$	1.4
rigid boundaries	≈ 1700	$\approx \pi$	≈ 1

Figure 5: Critical width ℓ_c of rolls for stress-free (above) and rigid (below) boundary conditions.

2 Examples of complex spatial patterns in convection

Actual Rayleigh-Bénard convection leads to straight rolls only at very low Rayleigh numbers and under carefully controlled conditions. Other possibilities are illustrated below.

2.1 Instabilities of straight rolls

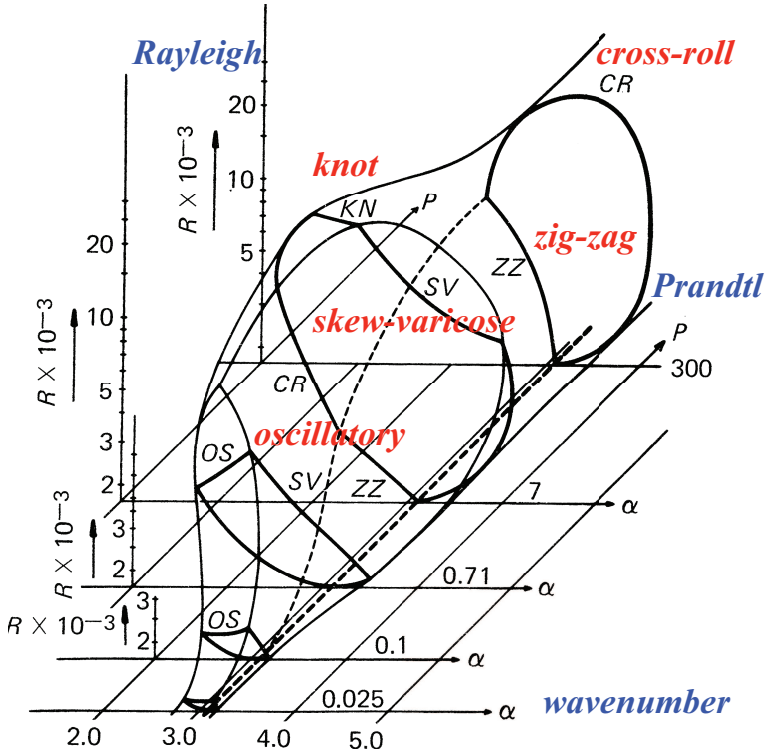

Figure 6: Instabilities of straight rolls. From *Transition to Turbulence in Rayleigh-Bénard Convection* by F.H. Busse. In *Hydrodynamic Instabilities and the Transition to Turbulence* ed. H.L. Swinney and J.P. Gollub, Springer 1981.

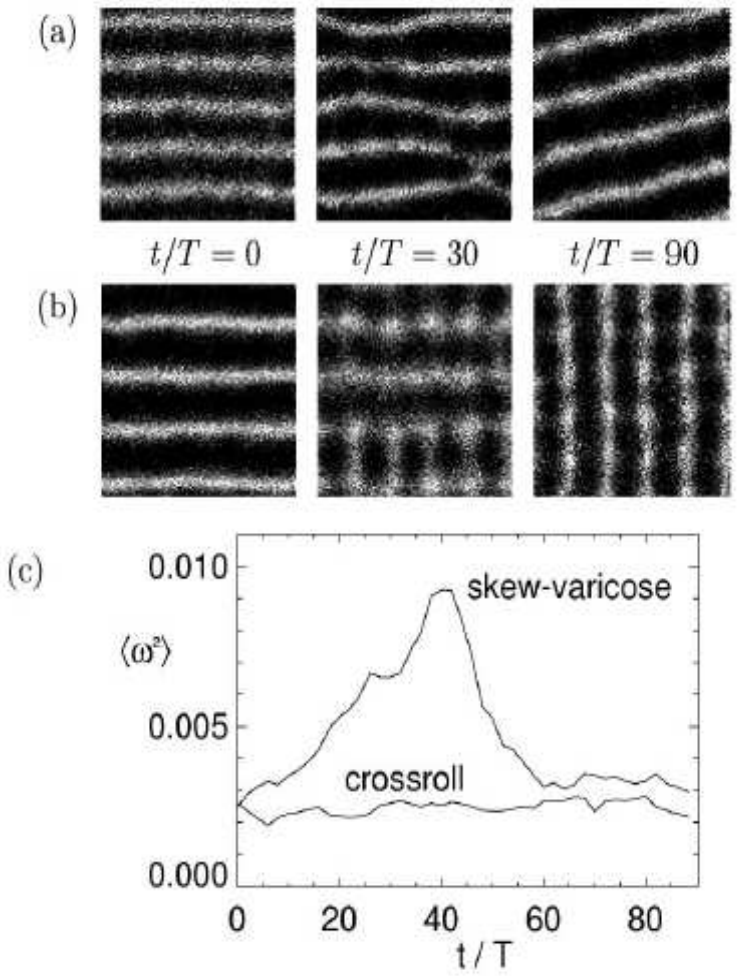

Figure 7: Instabilities of a striped pattern in a vertically-vibrated granular layer. Top: skew-varicose instability. Bottom: cross-roll instability. From J. de. Bruyn, C. Bizon, M.D. Shattuck, D. Goldman, J.B. Swift & H.L. Swinney, *Continuum-type stability balloon in oscillated granulated layers*, Phys. Rev. Lett. **81**, 1421 (1998).

2.2 Other patterns and flows

Figure 8: Spiral defect chaos in experimental convection. From Egolf, Melnikov, Pesche, Ecke, Nature **404**, 733-736 (2000).

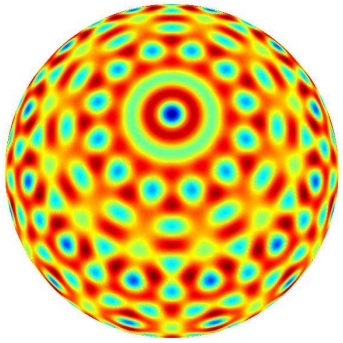

Figure 9: Convection pattern on sphere corresponding to spherical harmonic $\ell = 28$, constructed by P. Matthews. From Phys. Rev. E. 67, 036206 (2003); Nonlinearity 16, 1449-1471 (2003);

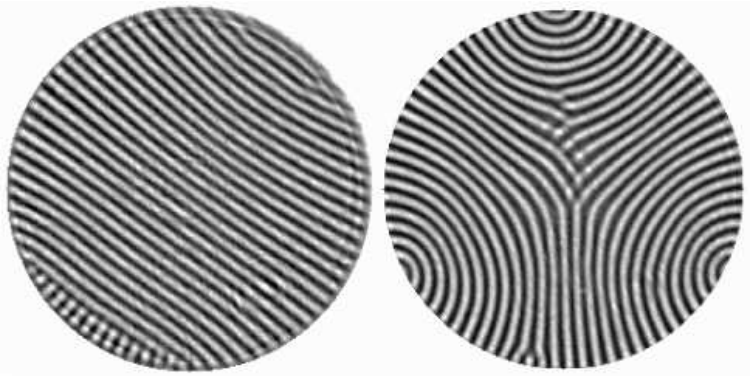

Figure 10: Convection in cylindrical geometry. From Bajaj, Mukolobwiez, Oh, Ahlers, J. Stat. Mech. (2006)

2.3 Convection in small containers

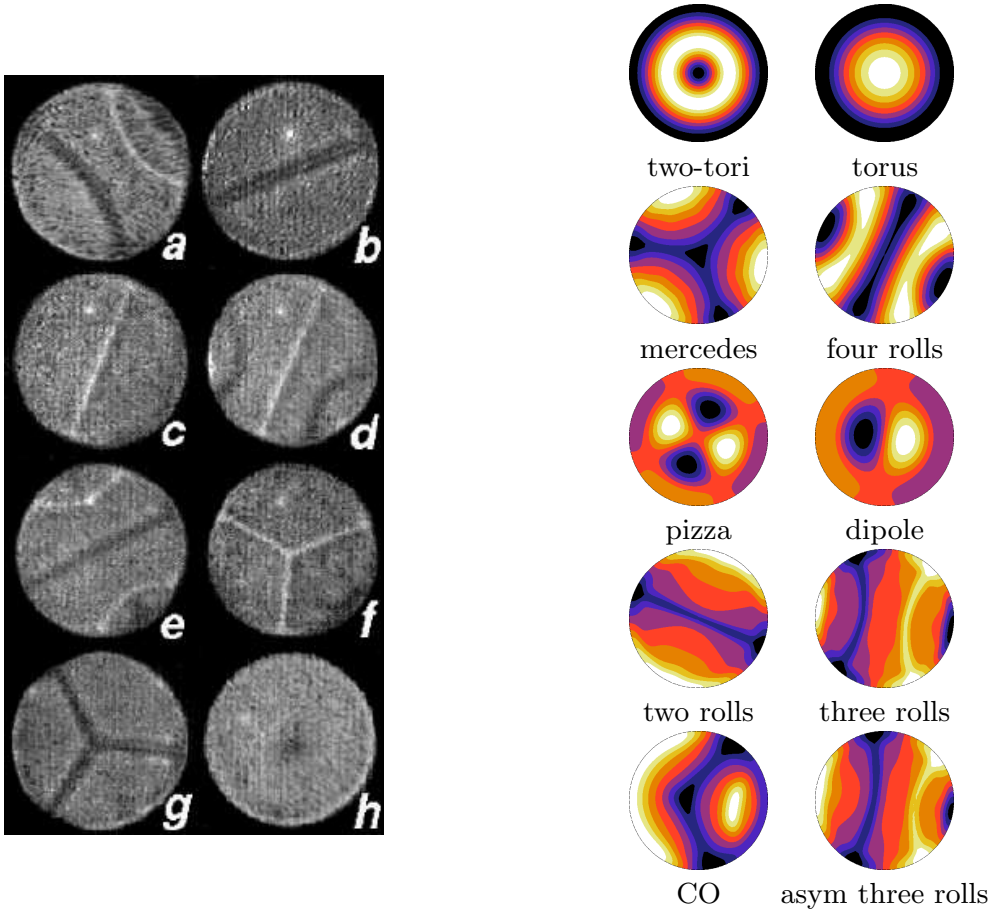

Figure 11: Left: experimental photographs of convection patterns in a cylindrical container whose radius is twice the height, all at the same Rayleigh number $Ra = 14\,200$ by Hof, Lucas, Mullin, Phys. Fluids **11**, 2815 (1999). Dark areas correspond to hot (rising) and bright to cold (descending) fluid. Right: numerical simulations by Borońska, Tuckerman, Phys. Rev. E **81**, 036321 (2010).

2.4 Geophysics

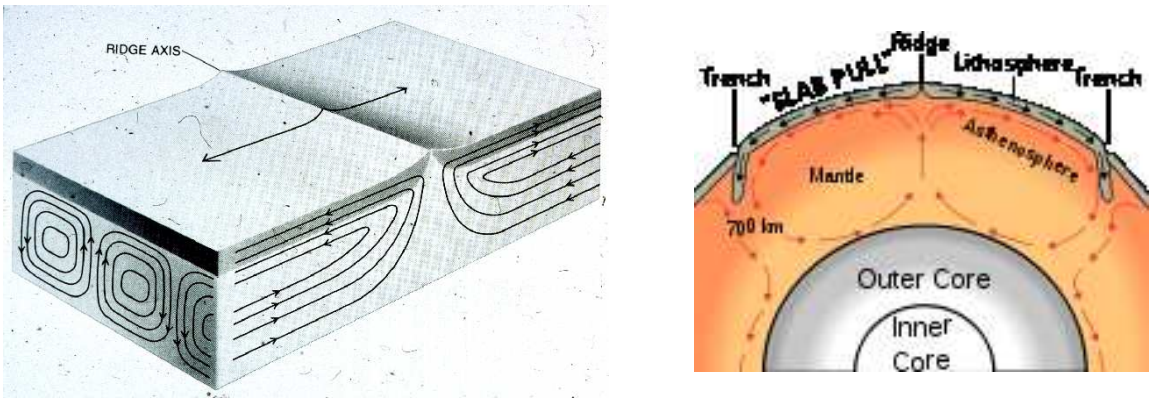

Figure 12: Convection and plate tectonics.

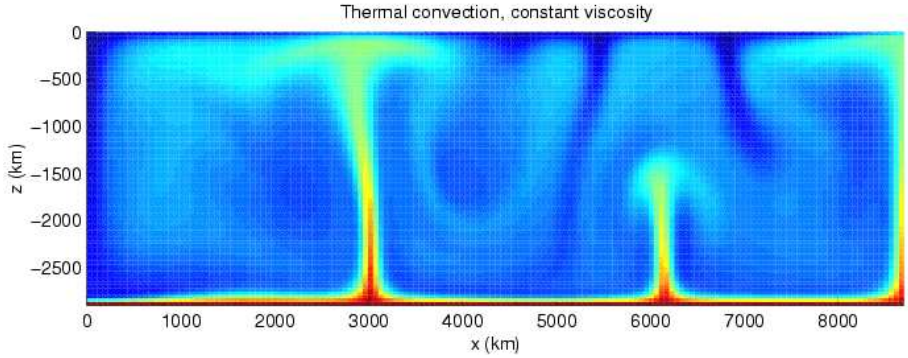

Figure 13: Numerical simulation of convection in the earth's mantle, containing plumes and thin boundary layers. By H. Schmeling, Wikimedia Commons. http://en.wikipedia.org/wiki/File:Convection-snapshot.gif

3 Lorenz Model

3.1 Including nonlinear interactions

We will now attempt to reintroduce the nonlinear terms missing from (23). We now insert the forms (24) in the Poisson brackets:

$$\begin{aligned} J\left[\psi,\Delta\psi\right] &= J[\psi,-\gamma^2\psi] = \partial_x\psi\ \partial_z(-\gamma^2\psi) - \partial_x(-\gamma^2\psi)\partial_z\psi = 0 && \text{(33a)}\\ J[\psi,T] &= \hat{\psi}\hat{T}[\partial_x(\sin qx\sin\pi z)\partial_z(\cos qx\sin\pi z) - \partial_x(\cos qx\ \sin\pi z)\partial_z(\sin qx\ \sin\pi z)]\\ &= \hat{\psi}\hat{T}q\pi\left[\cos qx\ \sin\pi z\ \cos qx\ \cos\pi z + \sin qx\ \sin\pi z\ \sin qx\ \cos\pi z\right]\\ &= \hat{\psi}\hat{T}q\pi\ (\cos^2 qx + \sin^2 qx)\ \sin\pi z\cos\pi z\\ &= \hat{\psi}\hat{T}\frac{q\pi}{2}\ \sin 2\pi z && \text{(33b)} \end{aligned}$$

(As previously, in the left-hand-sides of (33), ψ, T are functions of (x,z,t), while in the right-hand-sides, $\hat{\psi}$, $\hat{T}$ are scalar coefficients.)

We thus see that including the nonlinear term $J[\psi,\Delta\psi]$ has no effect, but that using the functional forms (24) is inconsistent with the nonlinear term $J[\psi,T]$.

Let us generalize the functional forms (24) to

$$\begin{aligned} \psi(x,z,t) &= \hat{\psi}(t)\sin qx\ \sin\pi z && \text{(34a)}\\ \hat{T}(x,z,t) &= \hat{T}_1(t)\cos qx\ \sin\pi z + \hat{T}_2(t)\sin 2\pi z && \text{(34b)} \end{aligned}$$

We have already calculated the nonlinear interaction between ψ and T_1. Let us do the same for ψ and T_2:

$$\begin{aligned} J[\psi,T_2] &= \hat{\psi}\hat{T}_2\ [\partial_x(\sin qx\sin\pi z)\partial_z(\sin 2\pi z) - \partial_x(\sin 2\pi z)\partial_z(\sin qx\ \sin\pi z)]\\ &= \hat{\psi}\hat{T}_2\ q\ 2\pi\ \cos qx\ \sin\pi z\ \cos 2\pi z\\ &= \hat{\psi}\hat{T}_2\ q\ \pi\cos qx\ (\sin\pi z + \sin 3\pi z) && \text{(35)} \end{aligned}$$

The term $(\cos qx\sin\pi z)$ is already included in (34b), but $(\cos qx\sin 3\pi z)$ is not. Introducing a term T_3 in (34b) would lead to more new terms, ad infinitum. This is a version of what is called the *closure problem* of the Navier-Stokes equations, or of nonlinear equations in general. In 1963, Lorenz suggested stopping at term T_2, keeping this as the minimal nonlinear term and neglecting the generation of term $(\cos qx\sin 3\pi z)$. Using (26), (33), (35), equations (22) thus become:

$$\begin{aligned} \partial_t\hat{\psi} &= Pr(q\hat{T}_1/\gamma^2 - \gamma^2\hat{\psi}) && \sin qx\sin\pi z && \text{(36a)}\\ \partial_t\hat{T}_1 + q\pi\hat{\psi}\hat{T}_2 &= Ra\ q\ \hat{\psi} - \gamma^2\hat{T}_1 && \cos qx\sin\pi z && \text{(36b)}\\ \partial_t\hat{T}_2 + \frac{q\pi}{2}\hat{\psi}\hat{T}_1 &= -(2\pi)^2\hat{T}_2 && \sin 2\pi z && \text{(36c)} \end{aligned}$$

Defining

$$X \equiv \frac{\pi q}{\sqrt{2}\gamma^2}\hat{\psi}, \quad Y \equiv \frac{\pi q^2}{\sqrt{2}\gamma^6}\hat{T}_1, \quad Z \equiv \frac{\pi q^2}{\sqrt{2}\gamma^6}\hat{T}_2, \tag{37a}$$

$$\tau \equiv \gamma^2 t, \quad r \equiv \frac{q^2}{\gamma^6}Ra, \quad b \equiv \frac{4\pi^2}{\gamma^2} = \frac{8}{3}, \quad \sigma \equiv Pr \tag{37b}$$

gives the famous Lorenz model:

$$\dot{X} = \sigma(Y - X) \tag{38a}$$

$$\dot{Y} = -XZ + rX - Y \tag{38b}$$

$$\dot{Z} = XY - bZ \tag{38c}$$

We can still see the hydrodynamic origins of these equations. The parameter σ is often set to 10, which is the Prandtl number of water. The parameter r is the Rayleigh number divided by the convection threshold, which we have previously calculated, so that the threshold is $r = 1$. The viscous or thermal damping can be seen in the last, negative, terms of each of the equations in (38). The nonlinear terms arise from advection.

3.2 Calculating bifurcations

Steady states of (38) satisfy

$$0 = \sigma(Y - X) \implies X = Y \tag{39a}$$

$$0 = -XZ + rX - Y \implies X = 0 \text{ or } Z = r - 1 \tag{39b}$$

$$0 = XY - bZ \implies Z = 0 \text{ or } X = Y = \pm\sqrt{b(r-1)} \tag{39c}$$

The steady states are therefore:

$$\begin{pmatrix} 0 \\ 0 \\ 0 \end{pmatrix}, \quad \begin{pmatrix} \sqrt{b(r-1)} \\ \sqrt{b(r-1)} \\ r-1 \end{pmatrix}, \quad \begin{pmatrix} -\sqrt{b(r-1)} \\ -\sqrt{b(r-1)} \\ r-1 \end{pmatrix}, \tag{40}$$

The Jacobian of (38) is

$$\begin{pmatrix} -\sigma & \sigma & 0 \\ r - Z & -1 & -X \\ Y & X & -b \end{pmatrix} \tag{41}$$

For the steady state $(X, Y, Z) = (0, 0, 0)$, this matrix becomes

$$\begin{pmatrix} -\sigma & \sigma & 0 \\ r & -1 & 0 \\ 0 & 0 & -b \end{pmatrix} \tag{42}$$

Figure 14: Convection rolls. The two configurations are dynamically equivalent and correspond to the transformation $(\psi, T_1) \to (-\psi, -T_1)$.

The matrix (42) is block-diagonal, so its eigenvalues are such that

$$\lambda_1 + \lambda_2 = Tr = -\sigma - 1 < 0 \tag{43a}$$
$$\lambda_1 \lambda_2 = Det = \sigma(1 - r) \tag{43b}$$
$$\lambda_3 = -b < 0 \tag{43c}$$

The steady state will therefore first be a stable node (for $0 < r < 1$), then a saddle (for $r > 1$). A pitchfork bifurcation takes place at $r = 1$ which creates the two new fixed points $X = Y = \pm\sqrt{b(r-1)}$, $Z = r - 1$. The occurrence of a pitchfork bifurcation is related to the symmetry between (X, Y, Z) and $(-X, -Y, Z)$: if (X, Y, Z) is a solution to (38), then so is $(-X, -Y, Z)$. This symmetry is in turn a consequence of the geometrical and physical symmetry which implies the equivalence of the two flows shown on figure 14.

For the states $X = Y = \pm\sqrt{b(r-1)}$, $Z = r - 1$, the Jacobian becomes

$$\begin{pmatrix} -\sigma & \sigma & 0 \\ 1 & -1 & \mp\sqrt{b(r-1)}X \\ \pm\sqrt{b(r-1)} & \pm\sqrt{b(r-1)} & -b \end{pmatrix} \tag{44}$$

whose eigenvalues are solutions to the cubic equation:

$$\lambda^3 + (\sigma + b + 1)\lambda^2 + (r + \sigma)b\lambda + 2b\sigma(r - 1) = 0 \tag{45}$$

Rather than calculating the solutions of (45), we seek eigenvalues λ corresponding to a bifurcation, i.e. with zero real part. We therefore substitute $\lambda = i\omega$, which yields:

$$-i\omega^3 - (\sigma + b + 1)\omega^2 + i(r + \sigma)b\omega + 2b\sigma(r - 1) = 0 \tag{46}$$

Separating the real and imaginary parts leads to:

$$-(\sigma + b + 1)\omega^2 + 2b\sigma(r - 1) = 0 \tag{47a}$$
$$-\omega^3 + (r + \sigma)b\omega = 0 \tag{47b}$$

which yields:

$$\begin{aligned} \frac{2b\sigma(r-1)}{\sigma+b+1} &= \omega^2 = (r+\sigma)b \\ 2b\sigma(r-1) &= (r+\sigma)b(\sigma+b+1) \\ 2b\sigma r - 2b\sigma &= rb(\sigma+b+1) + \sigma b(\sigma+b+1) \\ r = \frac{\sigma(\sigma+b+3)}{\sigma-b-1} &= 24.74 \text{ for } \sigma = 10,\ b = 8/3 \end{aligned} \tag{48}$$

Therefore, at $r = 24.74$, the two steady states each undergo a Hopf bifurcation, leading to oscillatory behavior. It can be shown that this bifurcation is subcritical, creating unstable limit cycles which exist for $r < 24.74$.

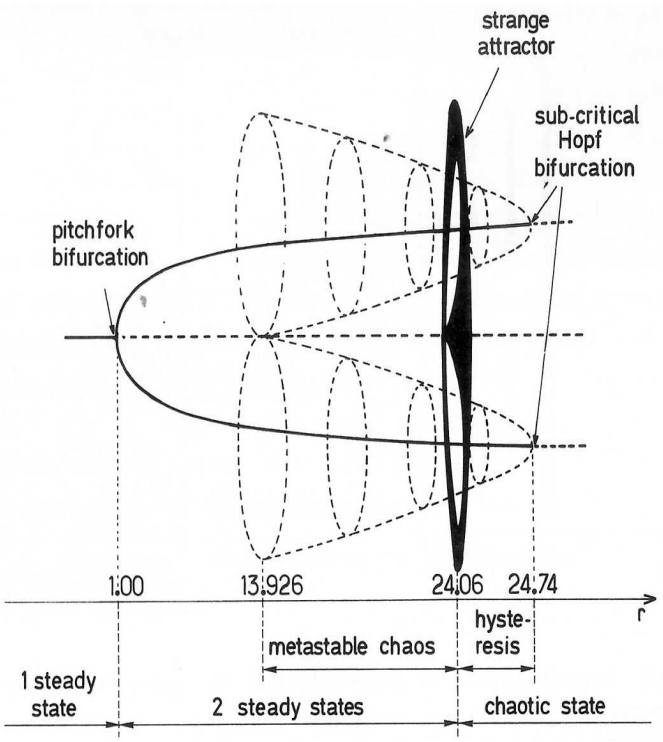

Figure 15: Bifurcation diagram for the Lorenz model for low $r \lesssim 25$, showing supercritical pitchfork and subcritical Hopf bifurcations. From *Order within Chaos* by P. Bergé, Y. Pomeau, C. Vidal, Wiley, 1986.

4 Some properties of the Lorenz model

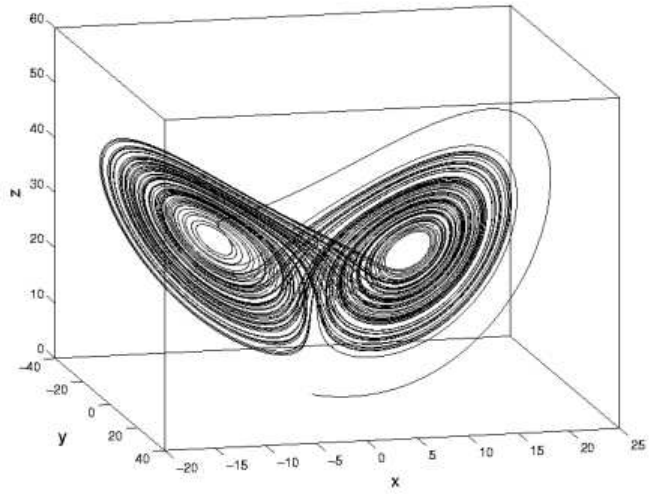

Figure 16: 3D view of chaotic Lorenz attractor at $r = 28$.

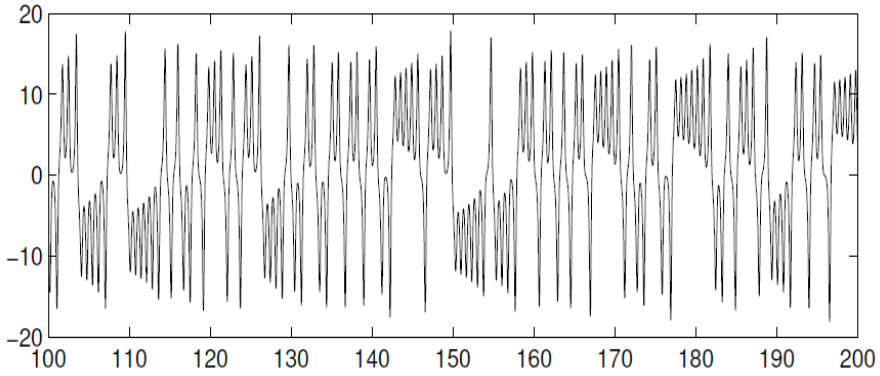

Figure 17: Timeseries $X(t)$ for Lorenz model at $r = 28$.

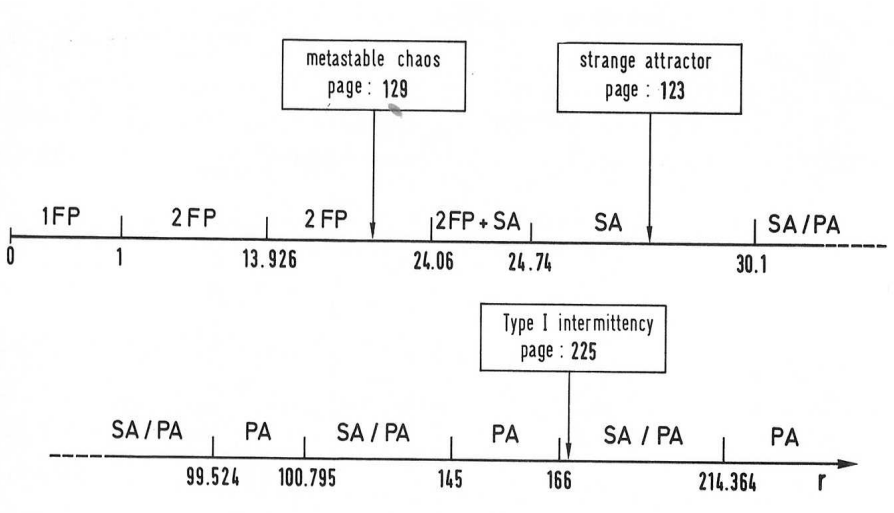

Figure 18: Regimes for the Lorenz model for $r \lesssim 220$, showing ranges of existence of fixed points (FP), strange attractors (SA), and periodic attractors (PA). From *Order within Chaos* by P. Bergé, Y. Pomeau, C. Vidal, Wiley, 1986.

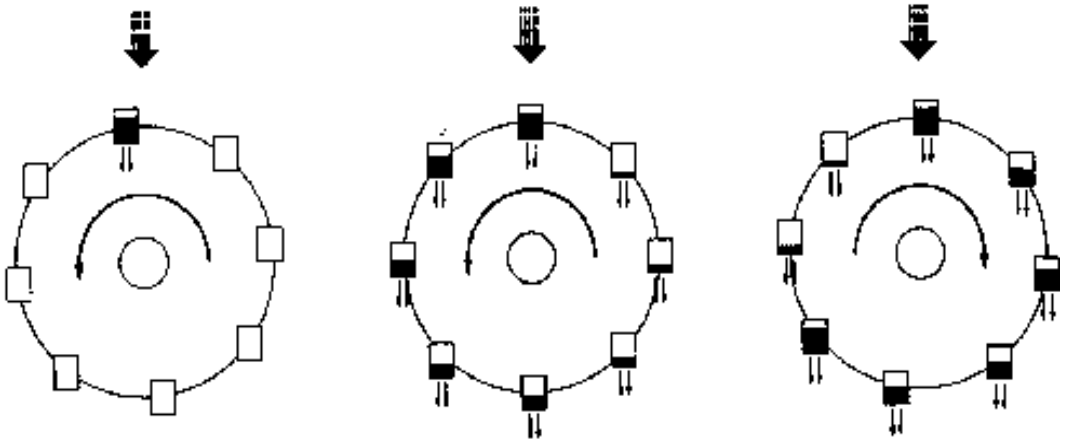

Figure 19: The Lorenz model does not provide a good description of Rayleigh-Bénard convection past threshold, but it does describe this waterwheel of leaking cups, proposed by W.V.R. Malkus.